Limnol. Oceanogr., 53(4), 2008, 1434–1445

Submarine discharge of nutrient-enriched fresh groundwater at Stinson Beach, California is enhanced during neap tides

Nicholas R. de Sieyes, Kevan M. Yamahara, Blythe A. Layton, Elizabeth H. Joyce, and Alexandria B. Boehm[1]
Environmental Water Studies, Department of Civil and Environmental Engineering, Stanford University, Stanford, California 94305-4020

Abstract

The influence of fortnightly spring–neap tidal variability on submarine discharge of fresh and saline groundwater was examined at Stinson Beach, California. Stinson Beach is a residential community that utilizes on-site systems for wastewater disposal. Fresh, shallow groundwater at the site contains high concentrations of nutrients (dissolved inorganic nitrogen [DIN], soluble reactive phosphate [SRP], and silicate) and human fecal bacteria. A groundwater-derived freshening and nutrification of the surf zone during neap tides was observed, followed by a 4-d increase in chlorophyll *a* concentrations. Analytical models and a freshwater budget in the surf zone were used to estimate the saline and fresh discharge of submarine groundwater. We estimate fresh groundwater discharge between 1.2 and 4.7 L min^{-1} m^{-1} shoreline during neap tides compared with 0.1 and 0.5 L min^{-1} m^{-1} during spring tides. This compares with 15.9 and 22.0 L min^{-1} m^{-1} saline groundwater discharge (forced by waves and tides) during neap and spring tides, respectively. Despite the smaller total (fresh + saline) flux of groundwater during neap compared with spring tides, the larger fresh discharge component during neap tides raises surf zone silicate, DIN, and SRP by 14%, 35%, and 27%, respectively, relative to spring tides. This observed fortnightly pulsing of fresh groundwater-derived nutrients was consistent with seaward hydraulic gradients across the fresh part of the beach aquifer, which varied due to aquifer overheight near the beach face. Darcy–Dupuit estimates of seaward fresh groundwater flow in this area agreed well with the fresh discharge results of the mass balance.

Submarine groundwater discharge (SGD), defined as fresh and saline groundwaters discharging along the coastline at the land–sea interface (Burnett et al. 2006), can contribute nutrients, metals, pollutants, and freshwater to the coastal environment (Johannes 1980; Bone et al. 2007). Driving forces of SGD include meteoric hydraulic head, tide and wave pumping, seasonal evapotranspiration cycles (Michael et al. 2005), and variations in groundwater density. Additional factors influencing the timing and magnitude of SGD include regional geology, climate, and human activities along the coast such as groundwater pumping and artificial recharge. The importance of combinations of factors controlling SGD vary from site to site, and site-specific studies are often required to fully understand SGD in a given region. Although a large body of literature has documented the existence and variability of SGD along the world's coastlines (Taniguchi et al. 2002), we are still working to understand the many factors that influence and modulate discharge rates.

Human activities along coasts can influence the quality of SGD (Kroeger et al. 2006). Nutrients emanating from fertilizers applied to residential lawns or agricultural fields may percolate through the vadose zone and increase concentrations in surficial aquifers (Valiela et al. 1992). In some coastal regions, households utilize cesspools or septic systems with leach fields for sewage disposal. These practices can recharge surficial aquifers with freshwater contaminated with pathogens, pharmaceuticals, nitrogen, and phosphorous (Robertson et al. 1991; Scandura and Sobsey 1997; Swartz et al. 2006). Several studies have investigated SGD in areas where on-site wastewater treatment is prevalent and have shown that SGD can contribute substantial nutrient loads to coastal waters (Giblin and Gaines 1990; Lapointe et al. 1990; Weiskel and Howes 1991). To protect human and ecosystem health, it remains important to continually improve our understanding of the magnitude and timing of SGD in areas where septic systems are used for wastewater disposal.

A limited number of studies have documented the importance of spring–neap tides on total SGD (Kim and Hwang 2002; Taniguchi 2002; Boehm et al. 2004) but not on the fresh component of SGD specifically. A single study (Campbell and Bate 1999) has examined fortnightly variations in fresh SGD. The present study explores the influence of the fortnightly spring–neap tidal cycle on submarine discharge of fresh groundwater from an unconfined, septic effluent-affected coastal aquifer in

[1] Corresponding author (aboehm@stanford.edu).

Acknowledgments

We acknowledge Eric Foote, Timothy Julian, Daniel Keymer, Holly Michael, Alyson Santoro, Gregory Shellenbarger, Sarah Walters, and Keeney Willis for assistance in the field and suggestions for improving the manuscript. Comments from two anonymous reviewers improved the manuscript.

This research was supported by the National Sea Grant College Program of the U.S. Department of Commerce's National Oceanic and Atmospheric Administration under NOAA grant NA04OAR4170038, project R/CZ-197, through the California Sea Grant College Program. E.H.J. was supported by the John D. Isaacs Marine Undergraduate Research Assistant Program at California Sea Grant and the Stanford Vice Provost for Undergraduate Education. The views expressed herein do not necessarily reflect the views of California Sea Grant.

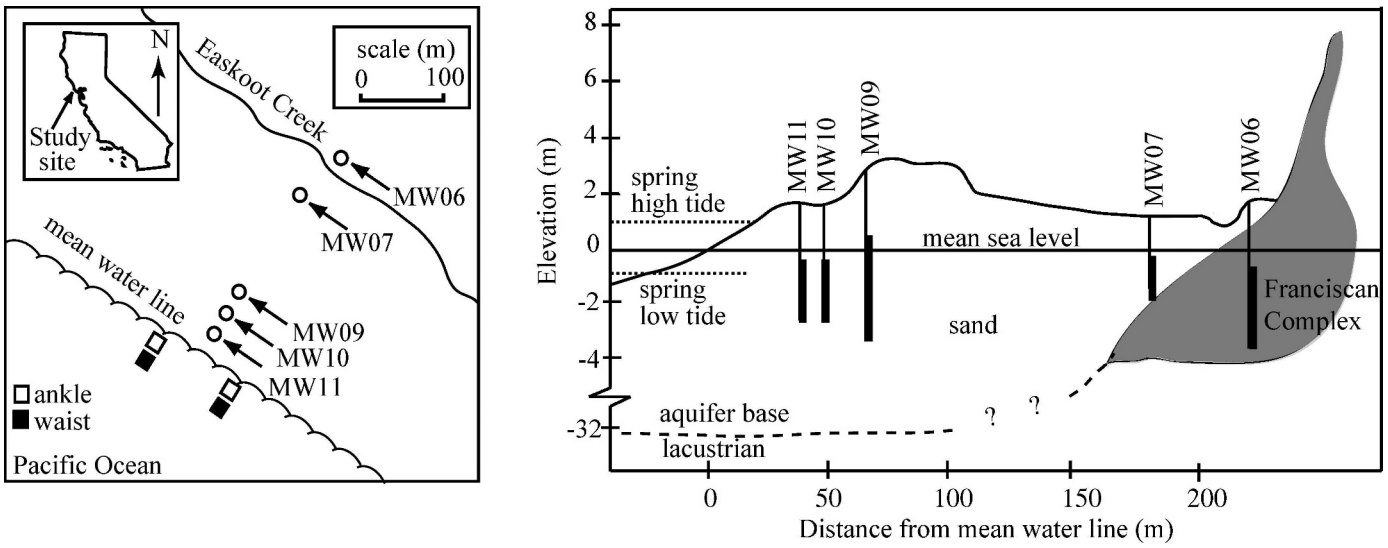

Fig. 1. Map of study area (left) and regional hydrogeology (right). Question marks in right panel indicate that contacts between geologic units in this region are uncertain.

Central California. Using a multifaceted approach that couples analytical models, hydraulic head measurements, and a nearshore freshwater budget, we document a neap tide pulsing of fresh, nutrient-enriched SGD. We link this enhanced neap tide discharge to fortnightly changes in seaward hydraulic gradient across the aquifer induced by aquifer overheight—the buildup or mounding of the water table near the land–sea interface as a result of tidal variation, wave setup, and wave run-up (Nielsen 1990; Turner et al. 1997; Horn 2006)—near the beach face. Using field data and a controlled mesocosm experiment, we explore the potential role of nutrient-enriched groundwater in causing increases of chlorophyll *a* (Chl *a*) in the coastal ocean at the site.

Methods and materials

Study site—Fieldwork was conducted from 14 through 28 July 2006 to characterize SGD from the unconfined aquifer over a spring–neap cycle at Stinson Beach, a small residential community 30 km north of San Francisco, California (37°53′58.387″N, 122°38′45.384″W, Fig. 1). The beach is an open-ocean, southwest-facing, reflective beach with mixed semidiurnal tides, a spring tide range of 2.4 m, typical breaker heights of 0.5–1.5 m, and a high energy surf zone. During the study, neap tide (17 July) preceded the spring tide (24 July).

The climate is Mediterranean with 60 to 120 cm of annual average rainfall occurring predominately between October and April (SBCWD 1998). During the dry season, Bolinas Lagoon (37°54′24.811″N, 122°40′54.732″W), a tidally influenced lagoon, and Webb Creek (37°53′7.332″N, 122°37′43.392″W), a nearby freshwater stream, are the only potential sources of fresh surface water to the nearshore marine environment within 7 km of Stinson Beach. There had been no precipitation in the watershed for approximately 2 months at the onset of the study, and no rainfall occurred during the study (data not shown). Easkoot Creek, a seasonal groundwater-fed creek, runs parallel to the shoreline through the field site approximately 200 m from the shoreline (Fig. 1). The creek discharges to Bolinas Lagoon and contains very little freshwater during the dry season.

Human development occupies 5% of the 29.3 km^2 Stinson Beach watershed and is primarily contained within 100 m of the coastline (geographic information system analysis not shown). Households use on-site septic systems and holding tanks exclusively for wastewater disposal. The areal density of standard gravity leach fields in the study area is approximately one leach field per 650 m^2 (SBCWD 1998).

The unconfined aquifer in the experimental area is composed primarily of beach and dune sands (Fig. 1, SBCWD 1998). At the beachhead, the sands are underlain by lacustrian clay at a depth of approximately 32 m below mean sea level (MSL) (Bergquist 1978). The unit overlies the Franciscan Complex, an assemblage of highly fractured sandstone, limestone, and shale (SBCWD 1998).

In systems with a high-energy surf zone, such as Stinson Beach, direct measurement of discharge with seepage meters is not possible (Libelo and MacIntyre 1994; Burnett et al. 2006). Breaking waves dislodge seepage meters and strong currents can induce flow through the seabed when passing over the objects (Huettel et al. 1996). This presents a unique challenge in the measurement of SGD in high-surf areas, and may explain the paucity of studies conducted on high-energy, open ocean coastlines in California and elsewhere. At Stinson Beach, we estimate SGD by combining three indirect methods: measurements of hydraulic head and Darcy–Dupuit calculations, a freshwater budget in the surf zone, and analytical models.

Hydraulic head measurements—Three permanent long-screen monitoring wells (MW06, MW07, and MW09) and two temporary piezometers (MW10 and MW11) were installed into the beach to create a cross-shore array (Fig. 1). Well construction details are shown in Table 1.

Table 1. Well construction details for the wells used in the study. Elevations are given in meters above mean sea level. Distances are given in meters from the mean water line.

Well ID	Diameter (cm)	Distance from mean water line (m)	Top of casing elevation (m)	Top of screen elevation (m)	Bottom of screen elevation (m)
MW06	10.16	223	1.46	−3.11	−4.63
MW07	10.16	178	1.36	−0.16	−1.69
MW09	10.16	70	3.10	0.05	−3.00
MW10	3.81	48	2.13	−0.92	−1.38
MW11	3.81	36	2.07	−1.13	−1.58

Beach topography and well elevations were surveyed relative to MSL. Measurements of hydraulic head were recorded in each well at 1-min intervals using pressure transducers (Solinst). The <1% of head measurements known to be misrepresentative of true aquifer conditions (hydraulic recovery after well installation and sampling) were removed and estimated by interpolation. All head measurements presented herein are presented as equivalent freshwater head. In the fresh part of the aquifer where hydraulic gradients are shallow (MW06 to MW09), the Dupuit assumptions are made. Namely, we assume that the hydraulic gradient is equal to the slope of the water table, and streamlines are horizontal and equipotential lines are vertical (Fetter 2001). Fortnightly average hydraulic heads at each well were calculated from head measurements collected during the entire experiment. Neap- and spring-tide head measurements were calculated by averaging measurements taken during the lunar day following the quarter (17 July) and new (24 July) moons, respectively.

Water sampling—At the low-low and high-high tide approximately every other day (n = 42 and 32, respectively), surf zone samples were collected at ankle and waist depths (0.2 and 0.7 m, respectively) along two cross-shore transects extending from the water line out into the surf zone adjacent to the well network (Fig. 1). Transects were approximately 100 m apart in the alongshore direction. At low-low tides only, the groundwater immediately adjacent to the water line was characterized by sampling from shallow pits dug into the beach approximately 10 m back from the water line (n = 19). In addition, subaerial seepage faces were sampled when they developed at the lowest tides (n = 17). Groundwater was sampled from the five wells approximately every 7 d ($2 \leq n \leq 5$ for each well). Surface offshore ocean water samples were obtained 180 m, 870 m, and 1,615 m from the shore in a cross-shore transect from our sampling site on the days of the third-quarter and new moons (n = 2 for each offshore location). The ebb flow from Bolinas Lagoon was sampled approximately every 4 d (n = 4). In all cases, clean, triple-rinsed 20-liter collapsible low-density polyethylene containers were used for water collection. A total of 100 liters for ocean and lagoon samples and 20–80 liters for groundwater samples were composited. A 1-liter subsample from large-volume samples was collected in clean triple-rinsed bottles and used for all chemical and biological analyses.

Tide elevation measurements were obtained from a National Oceanic and Atmospheric Administration tide gage at Point Reyes, approximately 30 km from Stinson Beach (http://tidesandcurrents.noaa.gov, Sta. ID 9415020, 37°59′48.12″N, 122°58′30″W). Data were recorded at 6-min intervals. Daily tidal range was calculated from daily maxima and minima.

Sand analysis for hydraulic conductivity (K_h) determination—A 2-m continuous core was collected near MW09, homogenized, and analyzed for grain size distribution using American Society for Testing and Materials standard C136. Hydraulic conductivity (K_h) was estimated from grain size distribution using the method of Hazen (1911).

Salinity, dissolved oxygen, and nutrient analysis—Salinity and dissolved oxygen were measured in situ using a hand-held probe (Hydrolab). Salinity is reported according to the unitless Practical Salinity Scale and is accurate to ±0.01. A 30-mL aliquot of each sample was filtered with 0.45-μm pore size filter and stored at −20°C for nutrient analyses. The concentrations of soluble reactive phosphate (SRP), silicate, nitrate, nitrite, and ammonia were measured by standard methods with a nutrient autoanalyzer (Lachat QuikChem 8000). Samples were diluted as necessary to be within the machine's detection limits for each nutrient. Concentrations reported herein reflect both the required sample dilution and the precision of the analytical method. Dissolved inorganic nitrogen (DIN) was determined by adding molar concentrations of nitrogen species. Five percent of nutrient samples were analyzed in duplicate.

Chlorophyll a analysis—Waist-deep seawater samples were analyzed in duplicate for chlorophyll *a* using a modified version of Environmental Protection Agency (EPA) method 445.0 (Arar and Collins 1997). Samples were filtered immediately after collection through Whatman GF/F glass filters and stored at −80°C. Samples were analyzed approximately 7 months after collection, longer than the EPA-suggested holding time of 3 weeks. We assume that negative effects related to holding time are distributed equally across all samples, allowing intrastudy comparison. During analysis, filters were added to 10 mL of 90% acetone in water, shaken vigorously for 60 s, and steeped at 4°C for 18 to 24 h. Samples were then centrifuged and the supernatant was analyzed on a fluorometer (Turner Designs), acidified, and reanalyzed, as specified in the EPA method. The precision, on the basis of analysis of duplicates, is 5%.

Mesocosm experiments—Experiments were conducted to assess whether the addition of fresh groundwater to seawater promoted increases in Chl *a*. Stinson Beach seawater, collected from within the surf zone, was filtered through a 250-μm sieve to remove large zooplankton grazers (Pederson and Borum 1996). Groundwater from MW09 was 0.2 μm filtered to remove particulates. Filtered groundwater was added to sieved seawater to final concentrations (v/v) of 0%, 4%, and 8%. Mesocosms were run in duplicate in 3.5-liter clear plastic bottles. Bottles

were spaced evenly under constant fluorescent light with illuminance 200 lm m^{-2} and incubated at 15°C for 2 d. Samples were collected and analyzed every 4 to 8 h via EPA method 445.0 for in vivo fluorescence. A subset of samples was also analyzed for in vitro Chl *a* by the same method. A best-fit curve was used to estimate the concentrations of Chl *a* from in vivo fluorescence for those samples for which only fluorescence had been measured. No more than 10% of bottle volumes was removed over the course of the experiment. Data collected on the final day of the experiment were averaged for determining final Chl *a* concentrations.

Fecal indicator bacteria analysis—Water samples were analyzed for fecal indicator bacteria to determine the degree of contamination by human waste. Fifty milliliters of each sample were collected in a sterile container, and immediately stored on ice. *Escherichia coli* (EC) and enterococci (ENT) were quantified from 10 mL of water diluted with 90 mL of Butterfield buffer (Weber Scientific) using Colilert-24 and Enterolert (IDEXX), respectively, within 6 h of collection. Tests were implemented in a 97-well format following manufacturer's direction and allowed for the detection of EC and ENT concentrations between 10 and 24,192 most probable number (MPN) $(100\ mL)^{-1}$. Note that the units MPN $(100\ mL)^{-1}$ are the standard units for reporting indicator bacteria concentrations in water. No duplicate samples were analyzed.

*Enterococcal surface protein (*esp*) gene analysis*—A subset of ENT-positive samples was analyzed for the *esp* gene, a putative human-specific marker in ENT (Scott et al. 2005). Media from positive IDEXX wells was removed using a 21 1/2 gauge needle and syringe, and pooled for each sample. One milliliter of pooled media was enriched in tryptic soy broth for 4 to 6 h at 41°C. DNAs were extracted from a 1-mL aliquot of enrichment media using QIAamp DNA Mini Kit (Qiagen). Polymerase chain reactions (PCRs) containing 3 μL of template were run using the conditions, primers, and buffers described by Scott et al. (2005), except we used Platinum Taq (Invitrogen). PCR products were run on a 1.5% agarose gel and stained with SYBR Gold (Invitrogen). Positive and negative PCR and extraction controls were run in conjunction with unknowns.

Data analysis—Pearson correlation coefficients (r_p) between measured parameters were determined using SPSS. Groups of data were compared using Student's *t*-test. Correlations were deemed significant if $p < 0.05$.

Flux calculations—Total SGD (D) can be expressed as $D = D_t + D_w + D_m + D_s + D_d$ (modified from Li et al. 1999) where D_t and D_w represent saline outflow from tidal- and wave-driven circulation of seawater through the beach aquifer, respectively, D_m represents SGD of meteoric and artificially recharged fresh groundwater, D_s represents saline SGD forced by the seasonal recharge–evapotranspiration cycle (Michael et al. 2005), and D_d represents the outflow of density-driven saline waters. We will not consider contributions from D_s or D_d in our estimates for D, and the reasons for and implications of these omissions will be discussed.

The outflow seepage rate driven by wave setup per unit alongshore distance, D_w, can be expressed as follows (Longuet-Higgins 1983):

$$D_w = K_h S_w L \tag{1}$$

where K_h is hydraulic conductivity of the beach aquifer media, S_w is the slope of the wave setup, and L is the surf zone width defined as the distance between the breaker line and the wave run-up line. Expressions for S_w and L can be calculated from the local oceanographic and geologic conditions including breaker height H_b, beach slope S_b, and wave period T_w (Li et al. 1999).

Li et. al. (1999) used Nielsen's solution predicting the height of the water table with time in response to tidal forcing to estimate the tidally driven groundwater outflow seepage rate per alongshore distance (D_t). The resulting discharge rate is tidally averaged, implies quasi-steady-state conditions, and should be viewed as a first-order approximation. Following Nielsen (1990, eq. 31) and Li et. al. (1999),

$$\begin{aligned} D_t = {} & \frac{n_e A}{\kappa T_t}\exp(-\alpha)(\cos(\alpha) - \sin(\alpha)) \\ & + \frac{\sqrt{2} n_e A^2}{s_b T_t}\exp\left(-\sqrt{2}\alpha\right)\cos\left(\sqrt{2}\alpha\right) \\ & + \frac{n_e A^2}{s_b T_t} \end{aligned} \tag{2a}$$

with

$$\kappa = \sqrt{\frac{n_e \omega}{2K_h H}} \tag{2b}$$

and

$$\alpha = \frac{\kappa A}{s_b} \tag{2c}$$

In Eq. 2a–c, A corresponds to the tidal amplitude, T_t the tidal period, ω the tidal frequency, n_e the effective porosity of the beach sand, and H the aquifer thickness.

Input parameters required for calculating D_w and D_t at our study site are as follows. Beach slope was calculated from surveyed beach topography ($s_b = 0.0378$). Tidal amplitude (A) was set to 0.80 m and 1.12 m for neap and spring tides, respectively. The tidal period ($T_t = 12.42$ h) and frequency ($\omega = 1.41 \times 10^{-4}$ rad s^{-1}) of the M_2 harmonic were used. During the study, the period of the dominant swell (T_w) was 9.6 s (http://cdip.ucsd.edu, Sta. ID 029). Breaking wave heights (H_b) were approximately constant during the study and estimated to be 0.8 m from observations in the field. Porosity was estimated to be 0.4 by displacement of a known volume of sediment in water in a volumetric flask; all porosity was assumed to be effective porosity (n_e). The hydraulic conductivity (K_h) of the sand was measured in the lab with aquifer material and determined to be 3.85×10^{-4} m s^{-1}, as described earlier.

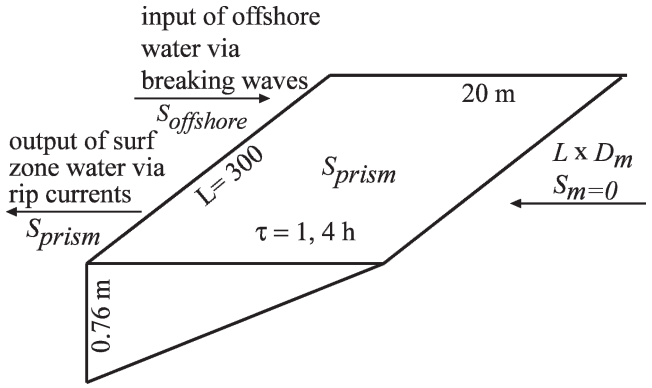

Fig. 2. Surf zone prism used as a control volume for the freshwater budget. Variables are defined in the text.

The unconfined aquifer thickness H was estimated to be 34 m from cores collected in the area, with an aquifer base approximately 32 m below sea level (Bergquist 1978; SBCWD 1998).

A mass balance was applied to the surf zone to calculate D_m at neap and spring tides using salinity as a tracer (Fig. 2). The surf zone adjacent to the well network was treated as a triangular prism with alongshore length (L) 300 m (typical distance between rip currents) and a right triangular cross-shore section of width 20 m (distance from shoreline to just beyond breakers) and offshore depth $20s_b$ (0.76 m). The salinity in the prism (S_{prism}) was determined for neap and spring tides by averaging all surf zone samples collected during the two lunar days before and after the quarter and new moons, respectively (two transects, both ankle and waist measurements, $n = 16$ and $n = 32$ for neap and spring tide, respectively). Although salinity measurements did not extend past 10 m in the offshore direction, surf zones are typically well mixed (Inman et al. 1971), so the calculated average salinity applied to the entire 20-m-wide prism. Water samples collected at 1,615 m offshore on the days of the third-quarter and new moons, which were the most saline and also the furthest from shore, were chosen as the offshore end member salinities ($S_{offshore}$). A salinity of 0 was assigned to the fresh groundwater end member. The following equation was used to estimate D_m per unit length of shoreline:

$$D_m = \frac{(S_{offshore} - S_{prism}) V_{prism}}{S_{offshore} L \tau} \quad (3)$$

where D_m is meteoric water flux in units of volume per time per unit length of beach, τ is the cross-shore residence time of water in the rip cell, L is the length of the shoreline of the prism (a single rip cell), V_{prism} is the volume of the prism, and S_{prism} and $S_{offshore}$ were defined previously. Following Boehm et al. (2004), we estimate the cross-shore residence time of water in a rip cell to be 1 to 4 h. Equation 3 assumes that D_m is small compared with the input of offshore waters into the surf zone via breaking waves (Fig. 2), and thus does not affect the water balance.

Estimation of fresh groundwater discharge across the land–sea interface is complicated by variations in fluid density, the existence of a seepage face, and the effects of tidal pumping. Our monitoring network is not as dense as would be needed for direct, accurate calculation of fresh and saline groundwater flux through the interface using Darcy's law. However, insight into the rate of fresh groundwater flow toward the land–sea interface, and thus the potential variation in freshwater discharge to the sea between neap and spring tides, can be provided by calculating groundwater flow through a landward section of unconfined aquifer using Darcy's law and the Dupuit assumptions (given previously), which are combined in the Dupuit equation (Fetter 2001):

$$Q' = -\frac{1}{2} K_h \left(\frac{h_1^2 - h_2^2}{Y} \right) \quad (4)$$

In Eq. 4, Q' is the flow per unit length of shoreline, K_h has been defined previously, and h_1 and h_2 are the saturated thicknesses at a distance Y apart. Flow was calculated between MW07 and MW09, the two furthest inland monitoring wells in the network installed in the unconfined aquifer, which are 178 and 70 m from the mean water line, respectively. The nature of the boundary between the unconfined aquifer and the highly fractured Franciscan Complex basement rock is uncertain, and for the purpose of this estimate we assume that the lacustrian clay at 32 m below MSL extends underneath the unconfined aquifer through this area, and that groundwater is fresh throughout the section. The flow through the landward part of the aquifer may not be exactly equal to D_m. Rather, since short-period (diurnal) tidal effects on head are small at MW07 and MW09 relative to effects of long-period (fortnightly) tides (data not shown), this flow rate can be thought of as the fresh groundwater entering the tidally pumped zone where density effects and vertical flow become important. It can also be considered a check on the mass balance-based estimates of D_m.

The "potential flux" (F_p) of nutrients to the surf zone via SGD was calculated as follows:

$$F_p = C_{fresh} D_m + C_{sal}(D_t + D_w) \quad (5)$$

where C_{fresh} and C_{sal} represent the end-member constituent concentrations in fresh and saline groundwaters, respectively. C_{fresh} and C_{sal} were estimated with mixing diagrams of salinity vs. nutrient for all groundwater samples (wells, pits, and subaerial seeps, $n = 55$), which were fit with a linear regression. The regression equation was extrapolated to fresh (0) and average offshore marine salinity (32.12) to determine C_{fresh} and C_{sal}, respectively. Multiplying groundwater end-member concentrations by SGD rates, as in Eq. 5, is a common method for estimating nutrient fluxes to the coastal ocean via SGD (Charette et al. 2001; Hwang et al. 2005*b*; Hays and Ullman 2007). However, the method assumes that the nutrient of interest behaves conservatively as it travels through the subsurface from aquifer to sea. In fact, sorption of SRP in groundwater systems is common (Slomp and Van Cappellen 2004) and the potential for nitrification and denitrification in the subterranean estuary has been demonstrated (Santoro et al. 2006, 2008). Therefore, Eq. 5 should be considered a first-order approximation of the true flux of nutrients.

Table 2. Arithmetic means for chemical concentrations and log-transformed bacterial concentrations in MPN (100 mL)$^{-1}$ for sample groups. Ninety-five percent confidence intervals are given in parentheses. For bacterial calculations, samples below the detection limit of 10 MPN (100 mL)$^{-1}$ were substituted with 5 MPN (100 mL)$^{-1}$. The *esp* gene column indicates how many of analyzed samples were positive.

Sample group	*n*	Salinity (-)	DO (mg L^{-1})	SRP (μmol L^{-1})	Silicate (μmol L^{-1})	log EC	log ENT	*esp* gene
MW06	4	0.22 (0.00)	4.1 (0.6)	0.7 (0.0)	409 (31)	0.7 (0)	0.7 (0)	-
MW07	4	0.97 (0.30)	1.5 (0.3)	9.2 (4.0)	447 (50)	4.38 (0)	4.38 (0)	2 of 4
MW09	6	3.44 (3.87)	2.5 (0.9)	18 (3)	436 (29)	3.48 (0.74)	2.29 (0.91)	-
MW10 & MW11	5	11.86 (5.84)	3.0 (0.2)	16 (17)	230 (77)	1.45 (0.49)	1.19 (0.69)	-
Pits	19	31.75 (0.24)	3.4 (0.2)	2.8 (0.1)	141 (8)	0.82 (0.09)	1.14 (0.3)	3 of 3
Seeps	17	30.22 (1.39)	5.8 (0.1)	2.4 (0.2)	102 (9)	0.79 (0.08)	0.82 (0.14)	-
Surf zone	84	32.02 (0.05)	6.6 (0.1)	1.7 (0.1)	44.9 (1.2)	1.08 (0.1)	0.96 (0.1)	0 of 2
Offshore	6	32.09 (0.09)	7.0 (0.5)	1.6 (0.2)	40.8 (3.2)	N/A	N/A	-
Bolinas Lagoon	4	32.34 (0.51)	6.0 (0.9)	1.6 (0.1)	45.9 (3.5)	2.32 (0.45)	1.29 (0.88)	1 of 1

Sample group	*n*	NO_3^- (μmol L^{-1})	NO_2^- (μmol L^{-1})	NH_3 (μmol L^{-1})	DIN (μmol L^{-1})
MW06	4	76 (2)	0.0 (0.0)	1.1 (0.6)	78 (2)
MW07	4	1.4 (1.6)	1.9 (2.4)	530 (80)	530 (80)
MW09	6	8 (4)	0.3 (0.0)	36 (70)	44 (66)
MW10 & MW11	5	160 (110)	7.6 (6.4)	40 (34)	210 (80)
Pits	19	21 (6)	4.0 (1.0)	2.4 (1.2)	27 (5)
Seeps	17	14 (5)	2.6 (1.0)	5.3 (1.8)	22 (5)
Surf zone	84	15 (1)	0.4 (0.0)	4.1 (0.4)	19 (1)
Offshore	6	14 (3)	0.3 (0.0)	3.1 (0.6)	18 (3)
Bolinas Lagoon	4	11 (1)	0.3 (0.0)	4.5 (1.7)	16 (2)

We used the calculated nutrient discharge values (F_p) to examine if observed changes in surf zone nutrient concentrations could be attributable to SGD. The following expression, which includes mass fluxes from all SGD components, excluding D_s and D_d, was used to predict the equilibrium concentration of DIN, SRP, and silicate in the surf zone, C_{prism}, under spring and neap tidal conditions:

$$C_{prism} = [C_{fresh}D_m + C_{sal}(D_w + D_t) + C_{offshore}(V_{prism}/\tau - D_m - D_w - D_t)] \quad (6)$$
$$(\tau/V_{prism})$$

D_m estimated from the freshwater budget was used. Surf zone residence times (τ) of 1 and 4 h were used. We then determined the predicted percentage change of each constituent in the surf zone during neap relative to spring tides and compared this with the constituent's actual change.

Results

Groundwater and coastal ocean water quality—The fresh groundwater in the unconfined aquifer at Stinson Beach contains high concentrations of fecal indicator bacteria, silicate, DIN, and SRP (Table 2). The presence of the *esp* gene in a subset of groundwater samples is consistent with their being affected by septic discharge (Table 2). A nutrient and fecal indicator bacteria-rich freshwater signature dissipates from inland wells (MW06, MW07, MW09) through the brackish mixing zone (MW10, MW11, pits and subaerial seeps) to the open ocean (surf zone and offshore samples). Fresh groundwater has, at most, 10, 130, 10, and 2,500 times higher silicate, DIN, SRP, and fecal indicator bacteria, respectively, compared with surf zone waters.

Tide range was positively correlated to salinity in the surf zone (Fig. 3, $r_p = 0.81$, $p < 0.01$), indicating a freshening of the surf zone during the neap tide. Tide range was negatively correlated to silicate, DIN, and SRP in the surf zone (Fig. 3, $-0.71 \leq r_p \leq -0.57$, $p < 0.01$, respectively), indicating nutrient enrichment in the surf zone during neap tides. Silicate, nitrate, DIN, and SRP concentrations were significantly negatively correlated to salinity (Fig. 3, $-0.73 \leq r_p \leq -0.49$, $p < 0.01$), supporting the idea that the freshening of the surf zone is caused by input of nutrient-enriched freshwaters and not by other large-scale saltwater nutrient sources such as upwelling, which can act on similar timescales.

The fresh component of discharges from Bolinas Lagoon and Webb Creek had little or no effect on the salinity in the surf zone at the experimental site. The salinity measurements taken during Bolinas Lagoon ebb flow were marine and were not significantly different ($p > 0.05$) from salinities in the surf zone at the study site. An 800-m alongshore transect of ankle-depth surf zone samples extending from the study site toward Webb Creek indicated that salinity was not decreasing with distance toward the creek (data not shown), indicating that the creek's freshwater plume does not substantially influence salinity of the surf zone at our site. Given these observations, we attribute the freshening of the surf zone during neap tides to discharge of fresh groundwater across the land–sea interface, and the corresponding nutrient increase a consequence of discharge of fresh groundwater to the coastal ocean from the surficial aquifer.

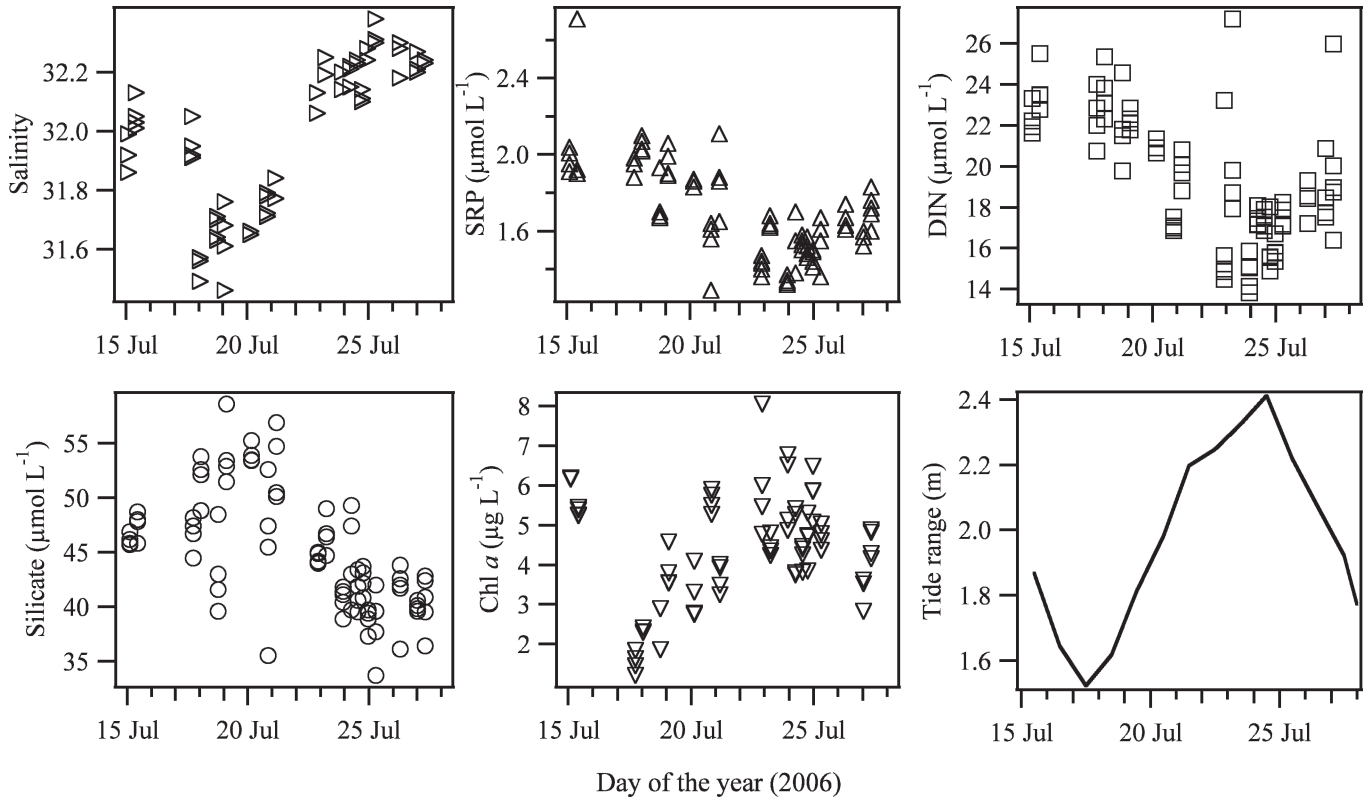

Fig. 3. Surf zone concentrations of salinity, SRP, DIN, SiO_4, Chl *a*, and tidal range plotted vs. time during the experiment.

Chl *a* concentrations in the surf zone increased substantially after the third-quarter moon. A least-squares regression of all Chl *a* measurements from 17 July (third-quarter moon) to 21 July with time ($r_p = 0.86$, $p < 0.05$) indicates an increase of over 1 μg L^{-1} d^{-1}.

Fecal indicator bacteria densities in the surf zone did not correlate significantly to salinity ($r_p = 0.16$, $p = 0.17$ for EC, and $r_p = 0.03$, $p = 0.79$ for ENT) or tide range ($r_p = 0.17$, $p = 0.13$ for EC, and $r_p = 0.01$, $p = 0.97$ for ENT). Despite the high concentrations of fecal indicator bacteria observed in fresh groundwater, they do not appear to be discharged with the fresh, nutrient-rich groundwater, indicating that they may be filtered as groundwater moves through the sand (Hijnen et al. 2005; Bolster et al. 2006).

Mesocosm experiment—Average Chl *a* with 95% confidence intervals at the start of the experiment (day 0, $n = 4$) and on the final day of the experiment (day 2, $n = 16$) are shown in Fig. 4. After incubation for 2 d, Chl *a* concentrations in bottles containing 4% and 8% groundwater exhibit significant ($p < 0.001$ in each case) increases relative to the seawater control. This experiment illustrates that a dissolved constituent present in the fresh groundwater at Stinson Beach, or a combination thereof, promotes the growth of phytoplankton in seawater when light and temperature are held constant.

Hydraulic head measurements—The head varied over a smaller range at the most inland wells compared with the wells closer to the sea (Table 3). The average hydraulic head over the fortnight at the well farthest from the sea, MW06, the only well installed into the bedrock at the landward boundary, the surficial beach aquifer, was higher than average heads at other wells installed into the beach

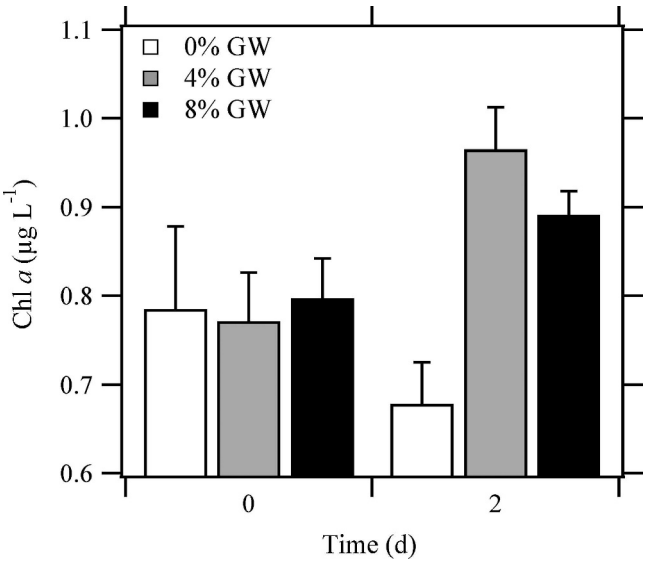

Fig. 4. Average and 95% confidence intervals of Chl *a* concentrations at time 0 and on day 2 of the mesocosm experiment for treatments (4% and 8% v/v groundwater and seawater) and control (0%). Concentrations in 4% and 8% treatments show significant increases above concentrations at time 0 and above control at day 2, suggesting that a dissolved constituent in groundwater is promoting growth of phytoplankton.

Table 3. The maximum and minimum equivalent freshwater hydraulic head (m) measured relative to mean sea level is shown for each well. Also shown are average heads during the fortnight, and during neap and spring tides. Sea level maximum, minimum, and average values are shown for comparison.

Well ID	Minimum (m)	Maximum (m)	Fortnight average (m)	Neap tide average (m)	Spring tide average (m)
MW06	1.26	1.39	1.32	1.33	1.28
MW07	0.41	0.55	0.48	0.49	0.44
MW09	0.24	0.56	0.42	0.37	0.44
MW10	0.08	1.03	0.45	0.26	0.55
MW11	0.08	1.01	0.43	0.39	0.49
Sea level	−1.28	1.18	0.09	0.11	0.18

aquifer (Table 3). This indicates that there was net flow from the bedrock to the surficial aquifer and out toward the sea, assuming a hydraulic connection. At the inland side of the unconfined aquifer, the hydraulic head in wells MW06 and MW07 was approximately 1 cm above the fortnight average during the neap tide and 4 cm below the fortnight average during the spring tide (Table 3). The reduction in head from neap to spring tide at these wells may be attributed to lagged response to low-frequency tidal constituents (Li et al. 2000; Raubenheimer and Guza 1999), or to the slow seasonal dropping of the water table during the summer months due to discharge and evapotranspiration. Changes to hydraulic head at the seaward side of the aquifer had an opposite and more substantial fortnightly trend. Neap tide average heads at wells MW09, MW10, and MW11 were 5, 19, and 4 cm below the fortnight averages, respectively, whereas spring tide heads at the same wells were 2, 10, and 6 cm, respectively, above the fortnight averages (Table 3). This illustrates an increase in aquifer overheight, or mounding of water at the land–sea interface during spring relative to neap tides.

SGD estimates—On the basis of the freshwater budget in the surf zone, D_m varies between 1.2 and 4.7 L min^{-1} m^{-1} of shoreline at neap tide to between 0.1 and 0.5 L min^{-1} m^{-1} at spring tide (range reported for 1- and 4-h residence times, Table 4). By comparison, estimates of discharge, on the basis of measurements in the fresh part of the aquifer, using the Dupuit equation are 1.2 L min^{-1} m^{-1} (neap tide) and 0.1 L min^{-1} m^{-1} (spring tide). Thus, agreement is excellent between the Dupuit freshwater discharge calculations and the mass balance estimates of D_m calculated with a 4-h residence time.

We calculate that D_w = 7.2 L min^{-1} m^{-1} of shoreline (constant throughout study) and D_t = 8.7 (neap) and 14.8 (spring) L min^{-1} m^{-1} of shoreline, respectively (Table 4). The sum of these estimates shows that total SGD (D) during spring tides (D_{spring}) is greater than SGD during neap tides (D_{neap}), which is consistent with results from other studies in unconfined aquifers, including those done with seepage meters (Kim and Hwang 2002; Taniguchi 2002; Boehm et al. 2004). Assuming a 1-h residence time, 2.2% of D_{spring} is fresh groundwater, whereas 22.8% of D_{neap} is fresh groundwater, or 0.5% vs. 7.0%, respectively, assuming a 4-h residence time (Table 4).

Discussion

Fortnightly trends in surf zone nutrients and salinity at Stinson Beach can be linked to changes in the meteoric (fresh) component of total SGD, which in this environment appears to be controlled by tide- and wave-driven aquifer

Table 4. (A) Dupuit equation estimates of seaward groundwater discharge in the fresh part of the unconfined aquifer. (B) Model estimates of D_m, D_t, D_w, D, F_p SiO_4, F_p SRP, and F_p DIN. Estimates vary for 1- and 4-h residence times. (C) Predicted C_{prism} for nutrients predicted using Eq. 6. Actual nutrient concentrations in the surf zone are reported for neap and spring tides for comparison.

(A)	Neap tide		Spring tide				
Fresh discharge (L min^{-1} m^{-1})	1.2		0.1				
(B)	Neap tide		Spring tide				
	1 h	4 h	1 h	4 h			
D_m (L min^{-1} m^{-1})	4.7	1.2	0.5	0.1			
D_w (L min^{-1} m^{-1})	7.2	7.2	7.2	7.2			
D_t (L min^{-1} m^{-1})	8.7	8.7	14.8	14.8			
D (L min^{-1} m^{-1})	20.6	17.1	22.5	22.1			
F_p SiO_4 (μmol min^{-1} m^{-1})	3,780	2,303	2,697	2,528			
F_p SRP (μmol min^{-1} m^{-1})	101	55	62	56			
F_p DIN (μmol min^{-1} m^{-1})	1,677	949	1,072	989			
(C)		Neap tide			Spring tide		
	1 h	4 h	Actual		1 h	4 h	Actual
C_{prism} Silicate (μmol L^{-1})	66	97	49		56	98	43
C_{prism} SRP (μmol L^{-1})	2.6	2.3	1.9		1.9	2.4	1.5
C_{prism} DIN (μmol L^{-1})	30	41	23		25	39	17

overheight in the unconfined beach aquifer. Increased fresh groundwater discharge at neap tide corresponded with a drop in aquifer overheight at the land–sea boundary and a steepening of the seaward hydraulic gradient in the fresh part of the aquifer. Similarly, increased aquifer overheight near the beach face during spring tide corresponded with a shallowing of the hydraulic gradient in the fresh part of the aquifer, and reduced fresh groundwater discharge to the coastal ocean. Fresh groundwater at the field site is substantially enriched in nutrients; thus the freshening of the surf zone during neap tide is accompanied by nutrification of the surf zone.

The discovery of fecal indicator bacteria and *esp*-positive ENT in monitoring wells at the site suggests that high nutrient concentrations in fresh groundwater are due at least in part to contamination by septic effluent. This is not surprising given the high density of septic systems at the field site. Our field observations indicate that nutrients from fresh groundwater can be transported from the land to the sea through the subsurface, affecting coastal water quality. Interestingly, increased surf zone concentrations of groundwater-derived nutrients were not associated with an increase in fecal indictor bacteria concentrations, although fresh groundwater at the site is enriched with these organisms. This indicates that attenuation of bacteria in the unconfined beach aquifer at Stinson Beach is efficient. Future work will concentrate on quantifying attenuation rates of effluent-derived fecal indicator bacteria, pathogens, in particular viruses, and nutrients in individual septage plumes at the site.

During the 4 d after the nutrient pulse that occurred at neap tide at Stinson Beach, Chl *a* concentrations in the surf zone increased from approximately 2 μg L^{-1} to 6 μg L^{-1}. Numerous studies have implicated SGD in causing algal blooms in the coastal ocean (LaRoche et al. 1997; Hwang et al. 2005*a,b*), with some specifically linking SGD-derived nutrient inputs from septic systems to growth of algae in canals and coastal watersheds (Lapointe et al. 1990; Valiela et al. 1992; Charette et al. 2001). The mesocosm experiments illustrated that the addition of nutrient-rich fresh groundwater from well MW09 (average nutrient concentrations in Table 2) to seawater promoted significant increases in Chl *a* relative to a control with no addition. Although we are unable to definitively conclude that nutrification of the coastal ocean by fresh SGD during the neap tide caused the increase in Chl *a* in the coastal ocean soon thereafter, our field observations and mesocosm experimental results are consistent with this linkage. Other possible causes of the increased Chl *a* in the surf zone include changes in resuspension of benthic diatoms (Demers et al. 1987), turbidity (May et al. 2003), water column stability and light penetration (Comeau et al. 1995), and upwelling (Labiosa and Arrigo 2003).

For the purposes of testing whether the observed changes in nutrient concentrations in the surf zone could have been caused by the estimated changes to SGD across the fortnight, theoretical spring- and neap-tide nutrient concentrations (C_{prism}) were estimated using the calculated potential nutrient fluxes (Eq. 5). On the basis of groundwater mixing diagrams of salinity vs. nutrient concentration, groundwater end-member nutrient concentrations were 422 μmol L^{-1} silicate, 208 μmol L^{-1} DIN, and 13 μmol L^{-1} SRP for fresh groundwater, and 113 μmol L^{-1} silicate, 44 μmol L^{-1} DIN, and 2.5 μmol L^{-1} SRP for saline groundwater (mixing diagrams not shown). Using these end members with the corresponding discharge estimates, the potential flux F_p ranges from 2,303 to 3,780 μmol min^{-1} m^{-1} silicate, 949 to 1,677 μmol min^{-1} m^{-1} DIN, and 55 to 101 μmol min^{-1} m^{-1} SRP, depending on residence time and tidal condition (spring vs. neap) (Table 4). Variation in F_p between neap and spring tides is due to the different proportions of D_m and D_t in total SGD (D).

Using F_p, we calculated C_{prism}, the theoretical concentration of nutrients in the surf zone during neap and spring tides. For each nutrient constituent C_{prism} is greater than the actual measured concentration in the surf zone during both tidal conditions (Table 4). This is not surprising given that nutrients do not behave conservatively in the subsurface, although our calculation of F_p assumes they do. However, comparisons of the projected change in C_{prism} between spring and neap tides with the actual change in surf zone concentrations agreed reasonably well assuming a 1-h residence time: C_{prism} increases 18% (silicate), 20% (DIN), and 37% (SRP) during neap relative to spring tides, as compared with the measured increases of 14% silicate, 35% DIN, and 27% SRP. Thus, it appears that if we use the low-end residence time estimate, the fortnightly changes in the flux of fresh and saline groundwater from the beach aquifer to the coastal ocean can account for an increase in surf zone concentrations of nutrients during neap tides. If the residence time is instead 4 h, then our model predicts higher nutrient concentrations during spring compared with neap tides presumably due to increased saline discharge at spring tide. This is counter to our observations, and may indicate that the nutrient flux attributed to the saline groundwater discharge is overestimated by our model.

Neither the seasonal component D_s nor the density-driven component D_d was included in flux calculations. Seepage metering was instrumental in investigating D_s at a low wave-energy field site at Waquoit Bay, Massachusetts (Michael et al. 2005). In systems with a high-energy surf zone such as Stinson Beach, seepage metering is problematic if not impossible (Libelo and MacIntyre 1994; Burnett et al. 2006), and for this reason D_s was not included in our estimate of D. However, since it oscillates on a yearly timescale, we can assume that D_s would have been approximately constant across the 14-d study. We contend that had D_s been included in our formulation of D, the percentages of fresh SGD of total reported above would be reduced but the relative differences and our general conclusions would remain the same. The variability and role of D_d at Stinson Beach is uncertain, but we suggest that because the fresh groundwater at the site is so substantially enriched in nutrients relative to the saltwater end members, the nutrification effects attributed to D_d variability would be small compared with those attributed by the large changes in fresh groundwater flux across the fortnight.

To ground-truth our discharge results, it is useful to compare them with those made in similar environments. At Tomales Bay, a 21-km-long embayment along the San Andreas Fault approximately 27 km to the northwest of Stinson Beach, Oberdorfer et al. (1990) estimated D_m using both Darcy's law and a soil moisture budget approach. Saline discharge was not investigated. D_m estimates for the two methods were 6.6×10^3 m^3 d^{-1} and 25.3×10^3 m^3 d^{-1}, respectively, or 0.12 L min^{-1} m^{-1} and 0.44 L min^{-1} m^{-1} given the approximate length of shoreline along the bay (40 km). During a multiday experiment, Mulligan and Charette (2006) used Darcy's law and radon-based methods and estimated fresh discharge to Waquoit Bay, Massachusetts, at 2.8 L min^{-1} m^{-1} and 3.9 L min^{-1} m^{-1}, respectively. Kroeger et al. (2007) used Darcy's law and a water budget to estimate fresh SGD from the Pinellas Peninsula in Tampa Bay, Florida. D_m was estimated at 2.0 L min^{-1} m^{-1} and 0.8 L min^{-1} m^{-1} using the two methods, respectively. Hays and Ullman (2007) dammed subaerial seepage faces that developed during 16 spring tide monitoring events across an 18-month period at Cape Henlopen, Delaware, and measured D_m directly with a weir. They calculated annual average D_m during the study of 0.9 ± 0.4 L min^{-1} m^{-1}. The range of D_m presented in our study is consistent with the values reported above.

SGD field studies have specifically investigated neap–spring tidal forcing of SGD. Taniguchi (2002) used seepage meters in Osaka Bay, Japan, and found that total SGD increased from neap to spring tide. At a monitoring station in Korea's Yellow Sea, Kim and Hwang (2002) found that groundwater-derived ^{222}Rn and CH_4 concentrations near the seafloor increased sharply from neap to spring tide. Boehm et al. (2004) also found an increase in total SGD between neap and spring tides using radium isotopes as tracers. In all three cases, the results indicate a greater total discharge during spring tide relative to neap tide, and are consistent with the results presented herein. The only study that examined spring–neap variation in fresh SGD, specifically, was conducted in South Africa. Campbell and Bate (1999) used a Darcy's law approach to quantify the flux of fresh groundwater from a South African sand dune complex, and estimated D_m to be 0.11 L min^{-1} m^{-1} during spring tide and 0.23 L min^{-1} m^{-1} during neap tide. The increase in neap tide D_m vs. spring tide D_m is also consistent with the results presented here.

The precise physical explanation of the neap tide pulsing phenomenon is unknown, though two numerical experiments have been conducted to examine D_m and D_t at a hypothetical beach under varying tidal amplitude scenarios and no wave action (Ataie-Ashtiani et al. 2001; Robinson et al. 2007), both of which offer some insights.

Ataie-Ashtiani et al. (2001) simulated constant-density steady-state D_m and D_t from a thin isotropic aquifer with a constant-head landward boundary under zero, low-, and high-tidal amplitude scenarios. They showed that increasing tidal range (as would be expected during spring tides) increased both D_t and aquifer overheight at the boundary, and decreased D_m. Despite differences between the simulated and Stinson Beach environments, the results of the simulation are consistent with the results of our study.

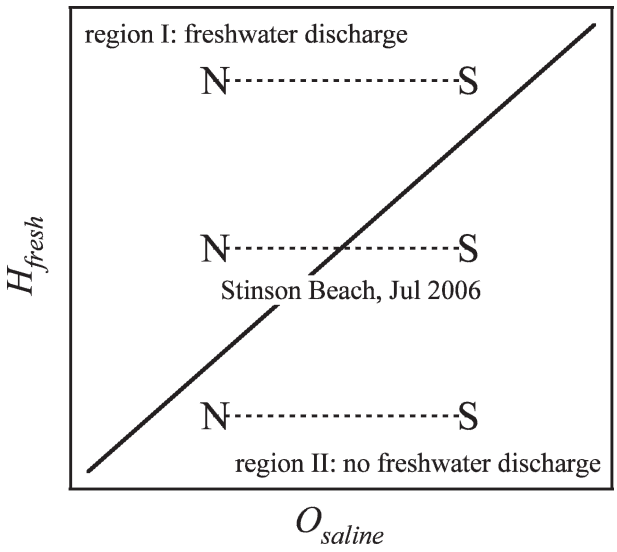

Fig. 5. A framework for understanding the timing of freshwater discharge at beaches similar to Stinson Beach. The dashed, horizontal lines connect the aquifer overheight (O_{saline}) during neap (N) and spring (S) tides at hypothetical beaches with varying hydraulic heads behind the overheight (H_{fresh}). The solid diagonal line separates regions I and II. In region I the aquifer overheight at the beach face is lower than the inland hydraulic head; fresh groundwater discharges to the coastal ocean. In region II, the aquifer overheight is higher than the inland hydraulic head; no freshwater discharge occurs. Fortnightly pulsed fresh groundwater discharge occurs when a beach straddles regions I and II.

Robinson et al. (2007) simulated variable-density steady-state D_m and D_t from a thick isotropic aquifer with a constant-flux fresh landward boundary and multiple tidal ranges. They showed that a saline tidally driven circulation cell develops approximately between the high and low tide lines. Under certain conditions, a freshwater "tube" discharges seaward of the tidal circulation cell near the low tide line. As tidal amplitude is increased, the depth and width of the saline circulation cell increase and the freshwater tube is forced to flow deeper in the aquifer and discharge further offshore. It is possible that during our study, fresh groundwater discharged to the surf zone at neap tide but discharged beyond the surf zone at spring tide, thereby producing a freshening of the surf zone at neap tide. Although we cannot rule out this possibility, no data collected at the site to date indicate a freshening of nearshore waters beyond the surf zone during spring tides (Table 2, additional data not shown).

Given the results described here, we present a qualitative framework for understanding the relationship between tide- and wave-driven overheight and the magnitude and timing of freshwater discharge from unconfined beach aquifers similar to that at our field site (Fig. 5). We introduce two variables, H_{fresh} and O_{saline}, where H_{fresh} is the hydraulic head in the fresh portion of the aquifer and O_{saline} is the hydraulic head due to overheight in the saline portion of the aquifer near the beach face. The magnitude of O_{saline} is controlled by several factors including wave setup, wave run-up, tidal height, and meteoric hydraulic pressure. H_{fresh} is measured just beyond the influence of

tides and waves and, thus, controlled entirely by meteoric hydraulic head.

In Fig. 5, O_{saline} (horizontal axis) is plotted against H_{fresh} (vertical axis). The dashed, horizontal lines represent neap (N) and spring (S) tide conditions at hypothetical beaches where H_{fresh} is relatively constant but O_{saline} varies with tide range, as it does at Stinson Beach. If H_{fresh} is higher than O_{saline} during all tidal conditions, the system is in region I of Fig. 5 and shallow fresh groundwater continuously discharges throughout the fortnightly tidal cycle. This may be the case at Waquoit Bay, a site with small tidal range and minimal wave action where researchers have described freshwater discharging to the coastal ocean under a variety of conditions (Michael et al. 2003; Mulligan and Charette 2006). If H_{fresh} is low relative to O_{saline} at both neap and spring tides, then shallow fresh groundwater does not discharge over the fortnightly cycle, and the system is in region II. This likely was the case in Huntington Beach, California (Boehm et al. 2006), where very little to no fresh groundwater discharge occurred despite the presence of fresh groundwater just landward of the high tide berm. At Stinson Beach, H_{fresh} is higher than O_{saline} during neap tide but lower during spring tide; thus, the system straddles regions I and II, resulting in a pulsing of fresh groundwater during neap tides with little or no discharge during spring tides.

It is conceivable that at Stinson Beach and elsewhere, aquifers may occupy regions I or II (or both) during different parts of the year as seasonal waves of meteoric hydraulic pressure force fresh groundwater though the beach and interact with the wave- and tide-driven overheight at the boundary. It is also conceivable that variable wave conditions across neap–spring cycles may interfere constructively or destructively with the neap–spring overheight cycle described herein. For these reasons and numerous others, we expect that not all tide- and wave-driven systems will fit into the above classification scheme. Future work including field experiments and numerical modeling will explore this concept more fully.

This study illustrates the importance of fortnightly variation in aquifer overheight in tide- and wave-driven systems and presents a qualitative framework for categorizing fresh groundwater discharge from beach aquifer systems similar to Stinson Beach with respect to overheight at the land–sea interface. Understanding the interactions of mechanisms forcing SGD is particularly important in systems similar to Stinson Beach, where fresh submarine groundwater discharge from a polluted unconfined aquifer poses potential risk to nearshore ocean ecosystem health. Further work should be done to examine the importance of neap–spring tides on submarine groundwater discharge in other environments.

References

Arar, E. J., and G. B. Collins. 1997. Method 445.0. In vitro determination of chlorophyll-a and pheophytin a in marine and freshwater algae by fluorescence. National Exposure Research Laboratory, Office of Research and Development, U.S. Environmental Protection Agency.

Ataie-Ashtiani, B., R. E. Volker, and D. A. Lockington. 2001. Tidal effects on groundwater dynamics in unconfined aquifers. Hydrol. Process. **15:** 655–669.

Bergquist, J. R. 1978. Depositional history and fault-related studies, Bolinas Lagoon, California. USGS Open-File Report 78-802.

Boehm, A. B., A. Paytan, G. G. Shellenbarger, and K. A. Davis. 2006. Composition and flux of groundwater from a California beach: Implications for nutrient supply to the surf zone. Cont. Shelf. Res. **26:** 269–282.

———, G. G. Shellenbarger, and A. Paytan. 2004. Groundwater discharge: A potential association with fecal indicator bacteria in the surf zone. Environ. Sci. Technol. **38:** 3558–3566.

Bolster, C. H., S. L. Walker, and K. L. Cook. 2006. Comparison of *Escherichia coli* and *Campylobacter jejuni* transport in saturated porous media. J. Environ. Qual. **35:** 1018–1025.

Bone, S. E., M. A. Charette, C. H. Lamborg, and M. E. Gonneea. 2007. Has submarine groundwater discharge been overlooked as a source of mercury to coastal waters? Environ. Sci. Technol. **41:** 3090–3095.

Burnett, W. C., and others. 2006. Quantifying submarine groundwater discharge in the coastal zone via multiple methods. Sci. Total Environ. **367:** 498–543.

Campbell, E. E., and G. C. Bate. 1999. Tide-induced pulsing of nutrient discharge from an unconfined aquifer into an *Anaulus australis*-dominated surf-zone. Water SA. **24:** 365–370.

Charette, M. A., K. O. Buessler, and J. E. Andrews. 2001. Utility of radium isotopes for evaluating the input and transport of groundwater-derived nitrogen to a Cape Cod estuary. Limnol. Oceanogr. **46:** 465–470.

Comeau, L. A., A. F. Vézina, M. Bourgeois, and S. K. Juniper. 1995. Relationship between phytoplankton production and the physical structure of the water column near Cobb Seamount, northeast Pacific. Deep Sea Res. I **42:** 993–1005.

Demers, S., J. C. Therriault, E. Bourget, and A. Bah. 1987. Resuspension in the shallow sublittoral zone of a macrotidal estuarine environment: Wind influence. Limnol. Oceanogr. **32:** 327–339.

Fetter, C. W. 2001. Applied hydrogeology, 4th ed. Merrill.

Giblin, A. E., and A. G. Gaines. 1990. Nitrogen inputs to a marine embayment: The importance of groundwater. Biogeochemistry **10:** 309–328.

Hays, R. L., and W. J. Ullman. 2007. Direct determination of total and fresh groundwater discharge and nutrient loads from a sandy beachface at low tide (Cape Henlopen, Delaware). Limnol. Oceanogr. **52:** 240–247.

Hazen, A. 1911. A discussion of ''Dams on sand foundations'' by A. C. Koenig. T. Am. Civ. Eng. **73:** 199–203.

Hijnen, W. A. M., A. J. Brouwer-Hanzens, K. J. Charles, and G. J. Medema. 2005. Transport of MS2 phage, *Escherichia coli*, *Clostridium perfringens*, *Cryptosporidium parvum*, and *Giardia intestinalis* in a gravel and sandy soil. Environ. Sci. Technol. **39:** 7860–7868.

Horn, D. P. 2006. Measurements and modeling of beach groundwater flow in the swash zone: A review. Cont. Shelf. Res. **26:** 622–652.

Huettel, M., W. Ziebis, and S. Forester. 1996. Flow-induced uptake of particulate matter in permeable sediments. Limnol. Oceanogr. **41:** 309–322.

Hwang, D., G. Kim, Y. Lee, and H. Yang. 2005*a.* Estimating submarine inputs of groundwater and nutrients to a coastal bay using radium isotopes. Mar. Chem. **96:** 61–71.

———, Y. Lee, and G. Kim. 2005*b*. Large submarine groundwater discharge and benthic eutrophication in Bangdu Bay on volcanic Jeju Island, Korea. Limnol. Oceanogr. **50:** 1393–1403.

Inman, D. L., R. J. Tait, and C. E. Nordstrom. 1971. Mixing in the surf zone. Geophys. Res. Lett. **76:** 3493–3514.

Johannes, R. E. 1980. Ecological significance of the submarine discharge of groundwater. Mar. Ecol. Prog. Ser. **3:** 365–373.

Kim, G., and D. Hwang. 2002. Tidal pumping of groundwater into the coastal ocean revealed from submarine ^{222}Rn and CH_4 monitoring. Geophys. Res. Lett. **29**, 1678, doi.10.1029/2002GL015093.

Kroeger, K. D., M. L. Cole, and I. Valiela. 2006. Groundwater-transported dissolved organic nitrogen exports from coastal watersheds. Limnol. Oceanogr. **51:** 2248–2261.

———, P. W. Swarzenski, J. Greenwood, and C. Reich. 2007. Submarine groundwater discharge to Tampa Bay: Nutrient fluxes and biogeochemistry of the coastal aquifer. Mar. Chem. **104:** 85–97.

Labiosa, R. G., and K. R. Arrigo. 2003. The interplay between upwelling and deep convective mixing in determining the seasonal phytoplankton dynamics in the Gulf of Aqaba: Evidence from SeaWiFS and MODIS. Limnol. Oceanogr. **48:** 2355–2368.

Lapointe, B. E., J. D O'Connell, and G. S. Garrett. 1990. Nutrient couplings between on-site sewage disposal systems, groundwaters, and nearshore surface waters of the Florida Keys. Biogeochemistry **10:** 289–307.

LaRoche, J., R. Nuzzi, R. Waters, K. Wyman, P. G. Falkowski, and D. W. R. Wallace. 1997. Brown tide blooms in Long Island's coastal waters linked to interannual variability in groundwater flow. Glob. Change Biol. **3:** 397–410.

Li, L., D. A. Barry, F. Stagnitti, and J.-Y. Parlange. 1999. Submarine groundwater discharge and associated chemical input to a coastal sea. Water Resour. Res. **35:** 3253–3259.

———, ———, ———, ———, and D. S. Jeng. 2000. Beach water table fluctuations due to spring-neap tides: Moving boundary effects. Adv. Water Resour. **23:** 817–824.

Libelo, E. L., and W. G. MacIntyre. 1994. Effects of surface-water movement on seepage-meter measurements of flow through the sediment–water interface. Hydrogeol. J. **2:** 49–54.

Longuet-Higgens, M. S. 1983. Wave set-up, percolation and undertow in the surf zone. Proc. R. Soc. Lond. A Mat. **390:** 283–291.

May, C. L., J. R. Koseff, L. V. Lucas, J. E. Cloern, and D. H. Schoellhamer. 2003. Effects of spatial and temporal variability of turbidity on phytoplankton blooms. Mar. Ecol. Prog. Ser. **254:** 111–128.

Michael, H. A., J. S. Lubetsky, and C. F. Harvey. 2003. Characterizing submarine groundwater discharge: A seepage meter study in Waquoit Bay, Massachusetts. Geophys. Res. Lett. **30:** 1297, doi:10.1029/2002GL016000

———, A. E. Mulligan, and C. F. Harvey. 2005. Seasonal oscillations in water exchange between aquifers and the coastal ocean. Nature. **436:** 1145–1148.

Mulligan, A. E., and M. A. Charette. 2006. Intercomparison of submarine groundwater discharge estimates from a sandy unconfined aquifer. J. Hydrol. **327:** 411–425.

Nielsen, P. 1990. Tidal dynamics of the water table in beaches. Water Resour. Res. **26:** 2127–2134.

Oberdorfer, J. A., M. A. Valentino, and S. V. Smith. 1990. Groundwater contribution to the nutrient budget of Tomales Bay, California. Biodegradation **10:** 199–216.

Pederson, M. F., and J. Borum. 1996. Nutrient control of algal growth in estuarine waters. Nutrient limitation and the importance of nitrogen requirements and nitrogen storage among phytoplankton and species of macroalgae. Mar. Ecol. Prog. Ser. **142:** 261–272.

Raubenheimer, B., and R. T. Guza. 1999. Tidal water table fluctuations in a sandy ocean beach. Water Resour. Res. **35:** 2313–2320.

Robertson, W. D., J. A. Cherry, and E. A. Sudicky. 1991. Groundwater contamination from two small septic systems on sand aquifers. Ground Water **29:** 82–92.

Robinson, C., L. Li, and D. A. Barry. 2007. Effect of tidal forcing on a subterranean estuary. Adv. Water Resour. **30:** 851–865.

Santoro, A. E., A. B. Boehm, and C. A. Francis. 2006. Denitrifier community composition along a nitrate and salinity gradient in a coastal aquifer. Appl. Environ. Microb. **72:** 2102–2109.

———, C. A. Francis, N. R de Sieyes, and A. B. Boehm. 2008. Shifts in the relative abundance of ammonia-oxidizing bacteria and archaea in a subterranean estuary. Environ. Microb. **10:** 1068–1079.

Scandura, J. E., and M. D. Sobsey. 1997. Viral and bacterial contamination of groundwater from on-site sewage treatment systems. Water Sci. Technol. **35:** 141–146.

Scott, T. M., T. M. Jenkins, J. Lukasik, and J. B. Rose. 2005. Potential use of a host-associated molecular marker in *Enterococcus faecium* as an index of human fecal pollution. Environ. Sci. Technol. **39:** 283–287.

Slomp, C. P., and P. Van Cappellen. 2004. Nutrient inputs to the coastal ocean through submarine groundwater discharge: Controls and potential impact. J. Hydrol. **295:** 64–86.

Stinson Beach County Water District (SBCWD). 1998. *Stinson Beach Hydrologic Survey*.www.stinson-beach-cwd.dst.ca.us.

Swartz, C. H., S. Reddy, M. J. Benotti, H. Yin, L. B. Barber, B. J. Brownawell, and R. A. Rudel. 2006. Steroid estrogens, nonylphenol ethoxylate metabolites, and other wastewater contaminants in groundwater affected by a residential septic system on Cape Cod, MA. Environ. Sci. Technol. **40:** 4894–4902.

Taniguchi, M. 2002. Tidal effects on submarine groundwater discharge into the ocean. Geophys. Res. Lett. **29:** 1561, doi:10.1029/2002GL014987.

———, W. C. Burnett, J. E. Cable, and J. V. Turner. 2002. Investigation of submarine groundwater discharge. Hydrol. Process. **16:** 2115–2129.

Turner, I. L., B. P. Coates, and R. I. Acworth. 1997. Tides, waves and the super-elevation of groundwater at the coast. J. Coastal Res. **13:** 46–60.

Valiela, I., and others. 1992. Couplings of watersheds and coastal waters: Sources and consequences of nutrient enrichment in Waquoit Bay, Massachusetts. Estuaries **15:** 443–457.

Weiskel, P. K., and B. L. Howes. 1991. Quantifying dissolved nitrogen flux through a coastal watershed. Water Resour. Res. **27:** 2929–2939.

Received: 29 July 2007
Accepted: 29 January 2008
Amended: 13 February 2008